

# Accepted Manuscript

Personal identification utilizing lip print furrow based patterns. A new approach.

Krzysztof Wrobel, Rafal Doroz, Piotr Porwik, Marcin Bernas

PII: S0031-3203(18)30163-8  
DOI: [10.1016/j.patcog.2018.04.030](https://doi.org/10.1016/j.patcog.2018.04.030)  
Reference: PR 6544



To appear in: *Pattern Recognition*

Received date: 1 November 2017

Revised date: 5 April 2018

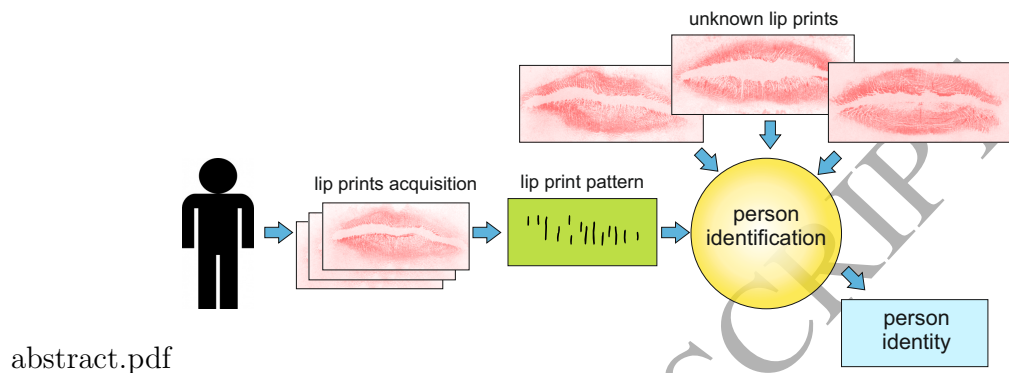
Accepted date: 27 April 2018

Please cite this article as: Krzysztof Wrobel, Rafal Doroz, Piotr Porwik, Marcin Bernas, Personal identification utilizing lip print furrow based patterns. A new approach., *Pattern Recognition* (2018), doi: [10.1016/j.patcog.2018.04.030](https://doi.org/10.1016/j.patcog.2018.04.030)

This is a PDF file of an unedited manuscript that has been accepted for publication. As a service to our customers we are providing this early version of the manuscript. The manuscript will undergo copyediting, typesetting, and review of the resulting proof before it is published in its final form. Please note that during the production process errors may be discovered which could affect the content, and all legal disclaimers that apply to the journal pertain.

## Highlights

- We propose a method to create the lip print pattern for each person.
- A novel method of directional lip furrows selection based on their size was proposed.
- The method focuses on the location and inclination of the furrows appearing on a lip print.
- We introduce a new measure of similarity between lip furrows.
- Our method achieves identification accuracy of 92.73%.

**Graphical abstract**

# Personal identification utilizing lip print furrow based patterns. A new approach.

Krzysztof Wrobel<sup>1</sup>, Rafal Doroz<sup>1</sup>, Piotr Porwik<sup>1</sup>, and Marcin Bernas<sup>2</sup>

<sup>1</sup>*Institute of Computer Science, University of Silesia, Bedzinska 39, 41-200 Sosnowiec,  
Poland*

<sup>2</sup>*Faculty of Mechanical Engineering and Computer Science, University of Bielsko-Biala,  
Willowa 2, 43-309 Bielsko-Biala, Poland*

{krzysztof.wrobel, rafal.doroz, piotr.porwik}@us.edu.pl,  
marcin.bernas@gmail.com}

## Abstract

This paper proposes a new method of personal identification that introduces the analysis of lip prints. In spite of its important role in forensic and biometric applications, the results of previous investigations into lip prints are scanty. This is mainly due to the difficulties that accompany any analysis of the lips: lips are very flexible and pliable, and successive lip print impressions - even those obtained from the same person - may significantly differ from one other.

Our article's principal contribution is a proposal for a new personal identification methodology and application that uses, for the first time, a strategy for biometric and forensic analysis of lip print structure. As a result of our analysis we propose a lip print pattern for each individual. This pattern contains only such furrows that occur on the greatest number of lip prints obtained from the same person, where these furrows' locations and inclinations remain similar across the lip prints obtained. It should be noted that in our approach, instead of lip photos we employ lip prints, such as can be obtained at a crime scene. It is worth noticing also that we propose a new method of personal identification where, instead of popular machine learning methods, the furrow-analysis of lip prints is introduced. Thus, no classifier learning phase is required. According to the authors' convictions, based on reports in the literature, the proposed approach describes for the first time a strategy as to how lip print structures could be analyzed in biometric applications.

The main novelty of this paper is its use of multiple lip print furrows from the same person to determine the most common lip furrow distribution in four different directions. On the basis of the pattern recognition of the lip furrows, the identity of the person will be determined. The proposed method's effectiveness is 92.73%, determined using a database containing 350 lip prints.

*Keywords:* Person identification, Lip print pattern, Forensics, Biometrics

## 1. Introduction

In the fields of forensic and criminal investigations, the identification of persons is always a challenge. In this context, fingerprinting and DNA techniques are probably the most popular approaches. However, these methods cannot always be used because criminals do not always leave their fingerprints behind at the crime scenes. Thus it becomes necessary to apply other identification techniques. Today, we know that not only fingerprints and footprints, but also hairs, the voice, blood, semen, DNA and clothes fibers can be treated as criminal identifiers. Some of these identifiers can be directly captured by police technicians at a crime scene. Many other pieces of evidence can be latent and, by the means of special chemical baths, fluorescent powders or floodlighting, can also be imaged [1, 2].

In 1932, Edmond Locard, a French criminologist, was the first who recommended the use of lip prints for personal identification [3]. Lip prints are the impressions of human lips left on objects such as drinking glasses, cigarettes, drink containers, aluminium foils, etc.

In the 1970s Yasuo Tsuchihashi and Kazuo Suzuki examined over 1000 samples of lip prints sourced from people of both genders, ranging from 3 to 60 years of age [4, 5]. Their investigations proved that lips characteristics (their dimensions and the topology of their patterning) were unique and unchangeably constant for each individual. In later years, these studies were continued by Jerzy Kasprzak. An outcome of his research was the identification and classification of 23 characteristic features appearing on the lips [6].

The collective name of the forensic investigation techniques in which human lip prints are analyzed is cheiloscopy [3]. The area of interest focused on by cheiloscopy is the system of furrows (bifurcations, crossings and other marks) on the human lips [7]. The uniqueness of lip prints makes cheiloscopy

especially effective whenever appropriate evidence is discovered at a crime scene, be it lipstick blot marks or lip prints left on cups, glasses or even on envelopes. Recently, in many countries, lip prints have been extensively used for determining an individual's sex or demographic characteristics, and even to identify the state within the country [8, 9]. In the papers cited, statistical analysis was performed on various types of lip prints, the analyses developed on the basis of cheiloscopy. Even though lip print analysis has not been substantially developed, this new form of identification is slowly becoming accepted and being introduced into practice worldwide. Nowadays, lip print analysis can be used for human identification, for example during a post-mortem examination [10]. It should be emphasized that cheiloscopy has already been successfully used as evidence in lawsuits [11].

No systems supporting the work of forensic technicians have yet been developed, and thus lip prints are analyzed manually. In this paper we propose a system that indicates which image or images of lips in a database is or are most similar to the lips being identified. This should speed up and facilitate the work of forensic technicians and allow them to at least obtain preliminary information about the person to be identified.

The lip prints discovered at a crime scene are often incomplete, are of low quality, and have been taken from a range of surfaces, all of which may negatively affect the process of lip print identification. Therefore, in this study, we have also conducted simulations on incomplete, low quality and deformed images. The solution proposed can be used in biometrics or forensics - two areas that are rapidly growing in importance. This paper is organized as follows: Section 2 discusses the use of lip prints as biometric and forensic features. Section 3 provides an overview of previous studies of the identification of persons based on their lip prints. The proposed identification method is described in Section 4, followed by experimental results and a discussion in Section 5. Finally, some conclusions are drawn in Section 8.

## 2. Lip print features

The surface of the lips is covered by numerous reticular depressions (furrows) that form a system of lines. The lips contain, on an average, 1145 individual features forming a unique pattern different for each person [5, 6]. This number is very large compared to a fingerprint, in which approximately 100 individual features can be identified. There is no doubt that the huge potential of the lips' patterns could bring extensive benefits in many domains e.g.

for personal identification [3, 12]. An early example of the use of lip prints for personal identification is a 1999 lawsuit in which the Illinois Appellate Court accepted the fact that "lip print identification is generally acceptable within the forensic science community as a means of positive identification" [11].

Identification or verification based on the lips requires that the lips' patterns are described by a set of features. Such features can be extracted from a photo of the lips or from a lip print. A lip print with sample features (furrows) is shown in Fig.1.

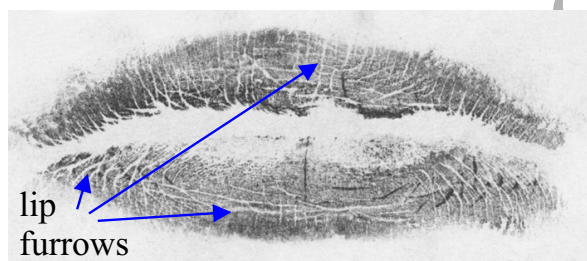


Figure 1: Lip print with sample furrows.

The features of the lips as extracted from photos have been used in various methods of biometric identification or in the verification of persons. However, these features are not used for the purposes of forensic analysis because the traces found at crime scenes are not photos of the lips but, rather, their prints. As a result, forensic analyses must be carried out using lip prints. In forensic laboratories, lip prints are transferred to special police materials by using a moisturizing cream, a roller with white paper, magnetic powder and a magnetic powder applicator. Their forensic analysis focuses on the location and inclination of the furrows occurring on a lip print. These techniques have been described by others in [6, 13]. Finally, the image appearing on paper is converted into a digital image by a scanner (Fig. 2).

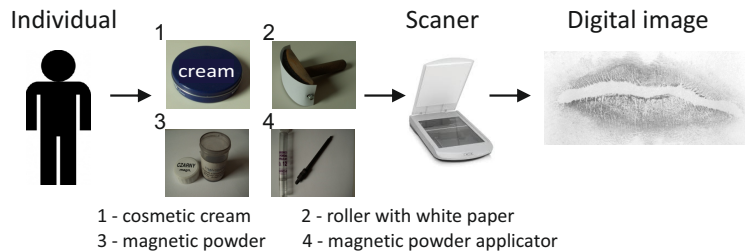


Figure 2: Stages of capturing a lip print.

### 3. Related work

Personal identification on the basis of the analysis of the lips is a relatively new area as compared to, for example, the analysis of fingerprints or handwritten signatures. However, in recent years, researchers have shown a significant increase of interest in this subject. In many studies a biometric approach has been proposed, consisting of an analysis of the geometric features of the lips as determined from photos [14, 15, 16, 17]. The features thus analyzed have included, for example, the length of the lips' contour, the surface area of the lips, and the width of the lips. The features determined were analyzed with the use of various methods such as Hidden Markov Models [18, 19], Multi-resolution architecture [20], Radon Transform [21], Zernike and Hu moment [22], PCA methods [18] and the SIFT technique [23]. Repositories of face images such as PIE, PUT, and MultiPIE were used most often as databases from which images of lips could be sourced [19].

Images of lips obtained from photos have also been used in recently popular multi-biometric systems [24]. Cetingul et al. in [25] proposed a system based on an analysis of the texture of the lips in a multimodal speaker recognition system, while Faraj and Bigun proposed an audio-visual personal authentication method using lip-motions obtained from orientation maps [26].

The remaining group of papers include studies on the identification and verification of lip prints [27, 28]. However, there are fewer such papers, which may be due to a lack of available databases in which there is a large number of lip prints of the same person. These are needed for the validation of the proposed method. We have developed such a database and made the images contained in it publicly available. All readers can now employ our database accessible via the website <http://biometrics.us.edu.pl>. A similar solution was proposed, inter alia, in [29], where a method for lip-based identification, based on a statistical analysis of furrows, was presented. The authors of that

work obtained an identification effectiveness at a level of 96%. However, it must be emphasized that that study was conducted on only twenty images. In [30], the author announced that the personal identification level was 58%, based on 300 lip prints. However, that database is not publicly available, so its characteristics are unknown in terms of their similarity to other works. In [31], identification of individuals reached a level of 78.37% on a basis of an analysis of 120 lip prints. In that investigation, only complete, clear and unblurred lip print were taken into consideration whereas, in this paper, blurred and incompletely defined lip images have been included. In our case, the acquisition of lip prints was performed at a different time (mainly over the period of one week) and imprints were taken under controlled pressure.

#### 4. Proposed method. The general idea

The proposed method of personal identification based on lip print images involves the creation of lip patterns and the subsequent identification of an unknown person's lips. The operation of this method is illustrated in Fig.3.

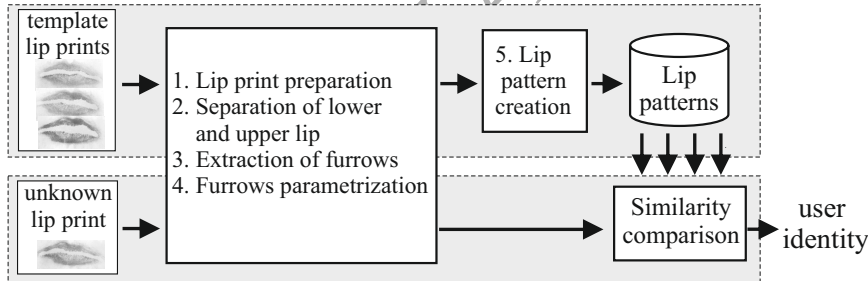


Figure 3: Flowchart showing the operation of the method.

A pattern is individually created for each person, a process involving five steps. In the first step, several lip prints are taken from each person and then appropriately prepared. In the second step, the prints are divided into upper and lower lips. During the third stage, the furrows on the separated lip images are made clearly visible. In the fourth step, a parameterization of the lip furrows is performed in which the length of the furrows as well as their locations and inclinations are established. The parameters to be measured are then determined from the lip patterns' vectors. In the last step, for each person, furrows are selected, the locations and inclinations of

which are similar across all lip prints collected from that individual. The selected furrows now comprise a lip print pattern for that person and are stored in the database.

The purpose of the identification stage is to identify the person from whom the lip print being evaluated was obtained. This print, after division into the upper and lower lips, the detection of furrows and their parameterization, is compared to the lip patterns of each person in the database. As a result of this identification, the print is classified as coming from the person whose pattern is most similar to it. A detailed description of the method is given in the following sections.

#### *4.1. Lip print preparation*

Lip print preparation takes place with the use of a white paper roller, magnetic powder and a magnetic powder applicator.  $N$  lip prints are taken from each person. All prints are collected on a sheet of paper having the same dimensions and then scanned and centered so that their location within the image is uniform. Subsequent steps of the lip print acquisition are presented in Fig. 2. In practice, lip prints can be deposited on a suitable surface in different directions, therefore each imprint has to be positioned within a Cartesian space. An appropriate orientation towards the OX axis is performed by means of the polynomial  $p(x) = p_1x^n + p_2x^{n-1} + \dots + p_nx + p_{n+1}$  of degree  $n$ . This will be discussed in the following part of the paper.

#### *4.2. Separation of the upper and lower lips*

In our proposed method, furrows are determined and then analyzed separately on each lip. For this purpose, each lip image is divided into the lower and upper lips. This procedure is carried out by adding a curve in the image running between the lips being separated. The part of the image above the curve includes the upper lip, while the remaining part of the image contains the lower lip. This method for dividing lip images into upper and lower lips was introduced in [30], but that method utilizes a so-called "brute force technique". As a result it's slow. In our work we employ a new approach in which a polynomial approximation is proposed for lip separation. Additionally, our technique, unlike the method of [30], obtains the correct result for both slightly open as well as closed mouths. After comparative studies, we concluded that our polynomial approximation gave better efficacy and was 65% faster.

In the first stage of the separation process, the image was subjected to binarization and dilatation which resulted in a better separation of the lip region from the background. The number of dilatation operations is denoted as  $\delta$  and will be estimated in the following experiments. The binarization was performed with the use of a method with an automatic selection of the binarization threshold [32, 33]. When analyzing the results of these operations it should be noted that binary artifacts may remain in the image. They might then be misinterpreted as elements of the lip region and consequently may hinder the division of the mouth into the upper and lower lips. Therefore they are removed from the image.

The operation of removing artifacts from the image begins by defining clusters of neighbouring black pixels in the image. Subsequently these will be referred to as pixel regions and denote as  $R$ . There are many pixel regions of different sizes in a lip image (Fig.4).

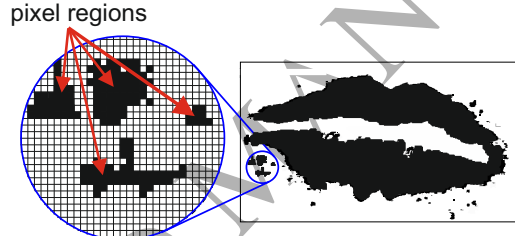


Figure 4: Examples of pixel regions that do not belong to the lips.

The size of each region is defined as the number of black pixels forming that region and is designated as  $\tilde{R}$ . All regions having a size smaller than a chosen threshold  $T$  are treated as artifacts and are removed from the image. The choice of threshold  $T$  is very important, as the removal of too large a region of pixels will destroy the structure of the original lip print, while the removal of too small a region will cause too many artifacts to remain visible. In the method presented here, the threshold value  $T$  is determined automatically for each lip print. The calculation of the value  $T$  begins with the creation of a histogram  $H$ . The histogram consists of  $n_{bin}$  bins  $H(i)$ ,  $i = 1, \dots, n_{bin}$ . Each bin  $H(i)$  determines the number of regions of a specified size in the image:

$$H(i) = \text{card}\{R_j : \tilde{R}_j \in (size_{min}, size_{max}] \} \quad i = 1, \dots, n_{bin}, \quad j = 1, \dots, n_{reg}, \quad (1)$$

where  $size_{min} = ((\tilde{R}^{\max}/n_{bin}) \cdot (i - 1))$  is the minimum size of the region  $R$  assigned to the  $i$ -th bin,  $size_{max} = ((\tilde{R}^{\max}/n_{bin}) \cdot i)$  is the maximum size of

the region  $R$  assigned to the  $i$ -th bin,  $n_{bin}$  is the number of histogram bins,  $\tilde{R}^{\max}$  is size of the largest pixel region in processed image and  $n_{reg}$  is the number of all regions in the image. The optimal  $n_{bin}$  value was evaluated experimentally and was checked in the range from 3 to 30. Ultimately, this parameter was set up to  $n_{bin} = 10$ . The higher value of this parameter did not improve the lip separation and negatively affects the processing time.

From the analysis of the histogram of any lip print image (Fig. 5) it can be observed, that the height of individual bins is smallest in the middle part of the histogram. This is a result of the fact that there are only very large and very small regions present in the image - respectively: regions of the upper and lower lip, and all artifacts surrounding the lips. Based on this observation, the threshold value  $T$  is determined as the number of the smallest bin and then rescaled to the size of the region corresponding to this bin (eq. 2). The regions with the number of black pixels greater than the threshold value  $T$  are treated as areas of the lower and upper lips. Remaining regions are removed from the image. The threshold value  $T$  is calculated through the use of the following formula:

$$T = \arg \min_i \{H[i]\} \cdot \frac{\tilde{R}^{\max}}{n_{bin}}, \quad (2)$$

where  $i = 1, \dots, n_{bin}$  is the number of bins.

An example of a lip print before and after removal of binary artifacts is shown in Fig.5.

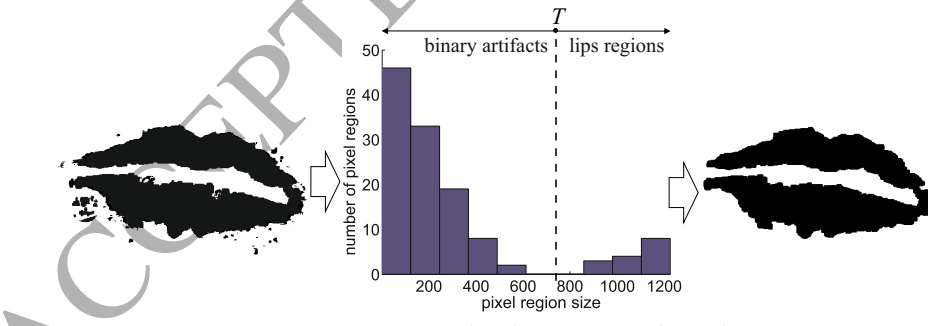


Figure 5: Lip print image before (left) and after (right) the removal of all artifacts (in presented example  $T = 720$  for  $i = 6$ ,  $\tilde{R}^{\max} = 1200$ ,  $n_{bin} = 10$ ).

In the next stage, the input image needs to be rotated towards the OX axis. This task requires determining the region between the lips. This is

accomplished by Algorithm 1 (see Appendix A). The algorithm analyzes each vertical line of the image and sets the black color for all pixels lying outside of the mouth shape (Fig. 6). It should be noticed that Algorithm 1 can be applied to both open as well as closed mouths.

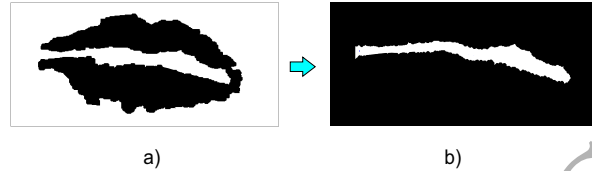


Figure 6: Input (a) and output (b) binary image after Algorithm 1.

Then, the obtained image (Fig. 7a) is then subjected to the process of skeletonization. The skeleton can be described as the set of  $(x, y)$  points, so that on the basis of this skeleton (Fig. 7b) the polynomial  $p(x)$  for  $n = 1$  is determined, where  $x$  stands for pixel-based skeleton points, and the best fit (in a least-squares sense) is achieved for  $y = p(x)$ . Fig. 7c) presents a lip image on the Cartesian plane together with a skeleton line and with its polynomial approximation as a straight line (polynomial  $p(x)$  for  $n = 1$ ). On the basis of the slope of the straight line, the angle  $\alpha$  between such a line and the OX axis can be determined and then, after a rotation of  $\alpha$ , the image will be appropriately positioned. Each input image is subjected to a rotating procedure specified by the steps depicted in Fig. 7.

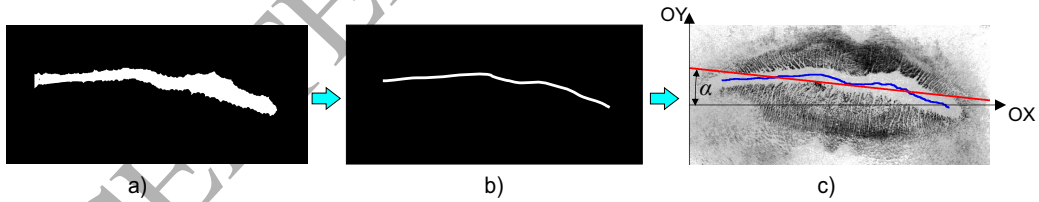


Figure 7: Input image preparation for orientation alignment. a) Result of Algorithm 1, b) skeletonized image, c) skeleton approximation as a straight line.

After mouth rotation, the next step is lips separation. On the basis of the same skeleton, an approximation by a quadratic polynomial ( $n = 2$ ) curve (Fig. 8b) is performed. This curve divides an input lip print image into images of the lower and upper lips (Fig. 8c). The quadratic polynomial appropriately maps the shape between the upper and lower lip images.

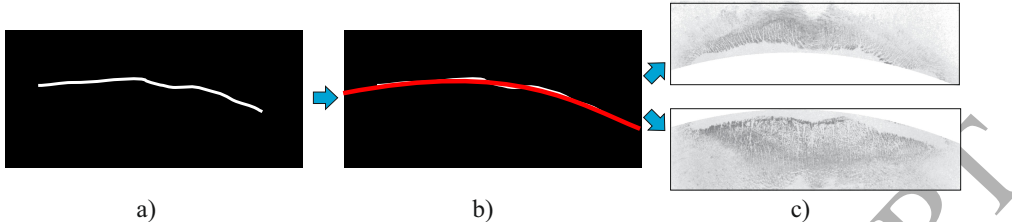


Figure 8: Process of division of the mouth into the lower and upper lips: a) skeletonized image, b) skeleton approximation by a quadratic polynomial ( $n = 2$ ) curve, c) images of separated upper and lower lips.

The other steps of the pattern creation process, including the extraction of furrows, their parameterization and the selection of furrows for the pattern, are carried out in the same manner for the upper and for the lower lips. For simplicity, in the remainder of this paper, these steps will be presented in a general way, without indicating the lip for which they were executed.

#### 4.3. The extraction of furrows from a lip print

The acquisition of furrows from a low-quality lip print may not be a simple task - for either an expert or as part of a fully automated process. Moreover, in the case of noisy or low-quality samples, fully automatic acquisition can generate false data. We have proposed a method in which the extraction of furrows is realized automatically. The most important steps of this process are presented in Fig. 9.

In the first step, the analyzed lip image is divided into its upper and lower parts by the method described in section 4.2. The number of dilatation operations used in this method is defined as parameter  $\delta$ . At this time only one selected part of the lip is processed (Fig. 9a). In the next step (Fig. 9b) an additional white background image is formed. In practice, the width and height of the background image are extended to the length of the diagonal of the image as seen in Fig. 9a. Then the analyzed image is shifted to the white background image and centered. In the future, this step will allow lip print rotation by various angles without any cutting of this image.

Next the normalization procedure is performed (Fig. 9c), where normalization means the stretching of the image's histogram (Fig. 9b).

In the following step only the lip region is extracted from the analyzed image (Fig. 9d). This is done by using the formulas (1) and (2). The image from Fig. 9d is then rotated (Fig. 9e) by the angle  $\alpha$  (implementation as described in [34]) and processed by a Gaussian convolution filter

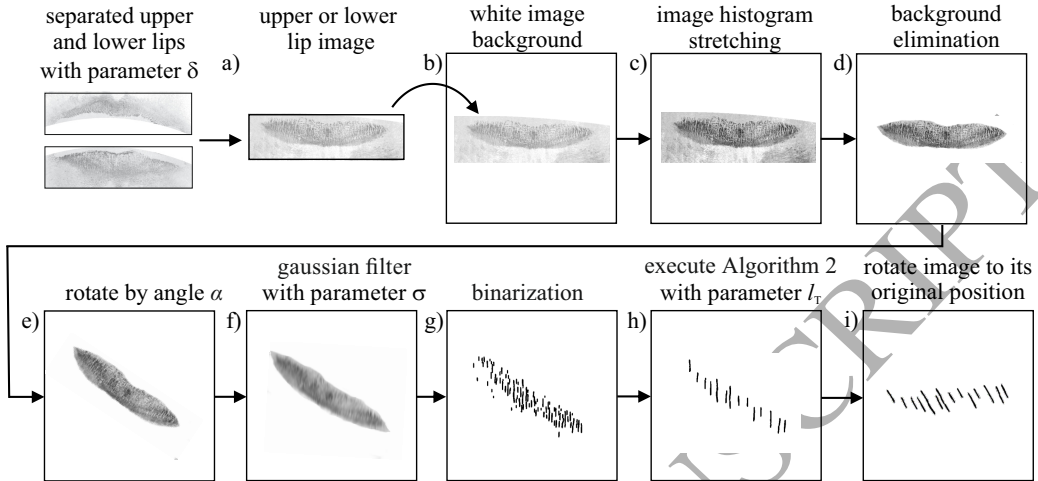


Figure 9: The lip print furrow extraction process.

$g[I(x, y), \alpha] = 1/2\pi\sigma^2 \exp(-(x^2+y^2)/2\sigma^2)$  (Fig. 9f) to strengthen the furrows in the direction  $\alpha$ , where  $\alpha \in \{-45^\circ, 0^\circ, 45^\circ, 90^\circ\}$ . From our experiments it was seen that such a range of angles was sufficient for analysis of the lip-based biometrics. Confirmation of this choice was shown experimentally, when the method's accuracy was checked, that it depends on a wide range of angles  $\alpha$ . The experiment's protocol will be shown later. This strategy was used due to its effectiveness, and because it allows a reduction in both the image's noise and in the number of details present [35].

Similarly to what has been described previously, the image depicted in Fig. 9f is then binarized using the same method as that in Section 4.2. The binarization results are presented in Fig. 9g. In the next step only those furrows that contain more than  $l_T$  pixels in total were selected (Fig. 9h). The parameter  $l_T$  was treated as a threshold level. To find the appropriate furrows, the length counting Algorithm 2 was proposed (see Appendix A). Finally, as presented in Fig. 9i, the lip print image was returned to its original orientation.

Algorithm 2 detects the furrows oriented in the vertical direction as in the Fig. 9h images. At first, the image is processed row by row: odd lines from left to right and even lines the opposite way (lines 4-7). In this way the size calculated in previous lane is propagated to next line and for each pixel of a given furrow the value 1 is added to the calculated sum (lines 8-17). Each of a furrow's pixels has a temporary label. At this step the last pixel of furrow

hold its size. By calculation, the size of a given furrow is determined and this size is distributed to each of the furrow's labels (lines 18-33). The distribution follows the path of previous iteration, but with opposite direction (lines 19-23). In the second part of the algorithm, the pixels with a label value below a given threshold ( $l_T$ ) are set to white, whereas those above the threshold are set to black (lines 34-39).

From the strategy as previously stated it follows that three parameters should be reliably estimated: the sigma ( $\sigma$ ) of the Gaussian filter, the furrow length ( $l_T$ ), and the number of dilatation operations ( $\delta$ ). In most cases, the expert is not able to perform this task, due to both the limits in his available time and because of the problem's complications. For this reason, we employ an evolutionary strategy to search for the optimal values in the space defined by those parameters. This requires multiple lip print samples obtained from the various person  $I_e$ ,  $e = 1, \dots, e_{max}$  as a reference. We propose using the Particle Swarm Optimization (PSO) method to solve this problem. The PSO algorithm was described first in [36] and its biometric implementations were discussed in our previous work [37].

The classification model employs expert reference decision (an expert manually identifies the furrows on a given lip print image), Algorithm 2 for the  $l_T, \sigma, \delta$  parameters and PSO method. The PSO parameters were set according to [38, 37]. Therefore, this paper will focus on the authors' contribution: the definition of the fitness function for  $l_T$  as well as the  $\sigma$  and  $\delta$  parameters. Each PSO particle is constructed as the tuple  $p_i = [l_T, \sigma, \delta]$ , where  $l_T = \{0, 1, \dots, 80\}$ ,  $\sigma = \{2, 3, \dots, 10\}$  and the number of dilatations  $\delta = \{0, 1, \dots, 8\}$ . The performance of each particle is measured using a fitness function  $f(p_i)$ :

$$f(p_i) = \frac{\sum_{e=1}^{e_{max}} \sum_{x=1}^{x_{max}} \sum_{y=1}^{y_{max}} I_e[x,y] \cdot I_i[x,y]}{\sum_{x=1}^{x_{max}} \sum_{y=1}^{y_{max}} I_e[x,y] \sum_{x=1}^{x_{max}} \sum_{y=1}^{y_{max}} I_i[x,y]}, \quad (3)$$

where  $I_i$  is an image with furrows marked by the furrow-finding algorithm based on  $p_i$  (Fig. 9) and  $I_e$  is the same image on which the furrows were selected by the domain expert.

In the theoretical approach, the function (3) reaches a value of 1 if all lip furrows are correctly located by the proposed method and where there are no additional artificially created furrows. In other words  $f(p_i) = 1$  means that the furrows identified on images  $I_i$  and  $I_e$  are identical.

The proposed approach was tested on ten particles with their initial values uniformly distributed over the search area, with the maximum number of iterations being 100. Increasing the number of particles did not improve the performance of the method. The experiments show that optimal PSO-based parameters are equal to  $l_T = 42$ ,  $\sigma = 5$  and  $\delta = 3$ . Thus these parameters are recommended for all further experiments. The PSO procedure was tuned on the basis of 40 separately prepared lip prints coming from 20 persons (2 prints per person). In future experiments, only lip prints from outside of the mentioned group of 40 images were taken into consideration. So, the proposed approach is person-disjoint.

In the last step, the analyzed image is rotated back to its original position (Fig. 9i).

The process of furrow extraction on each lip is carried out four times for different values of the angle  $\alpha \in \{-45^\circ, 0^\circ, 45^\circ, 90^\circ\}$ . The furrows obtained for different values of  $\alpha$  were shown in Fig. 10.

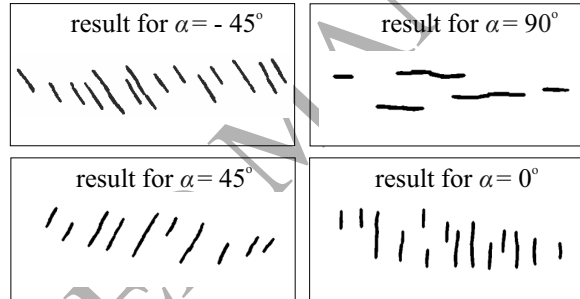


Figure 10: Other results of the method of finding furrows (Fig. 9i) for various values of the angle  $\alpha$ .

#### 4.4. Parameterization of the furrows in the image

The identification of lip prints is based on the patterns of furrows (wrinkles) on the lips. We can define many types of patterns such as lines, eyes, dots, etc. however, Suzuki and Tsuchihashi in [5] found that lines are the most frequent pattern. For this reason, this work focuses on the detection and analysis of straight lines that form a lip pattern. Thus, each furrow determined in the image is described by a vector  $\mathbf{L} = [x^{(u)}, x^{(d)}, \alpha, l]$ . Elements of the vector are found in the image by using the standard Hough Transformation (SHT) [39, 40], where  $x^{(u)}$  and  $x^{(d)}$  determine the coordinates  $x$  where the straight line passing through the furrow intersects with the upper

and lower edges of the image, respectively. The angle  $\alpha$  determines the inclination of the said straight line in relation to the  $OX$  axis. The parameter  $l$  is the length of the furrow expressed in pixels. Vectors  $\mathbf{L}$  are created only for those furrows that have a length greater than the value of the parameter  $l_T$  (see Algorithm 2). The parameters determined for different sample furrows are shown in Fig. 11 and Fig. 12. The  $x^{(u)}, x^{(d)}$  coordinates of the furrows are computed according to the furrows' location.

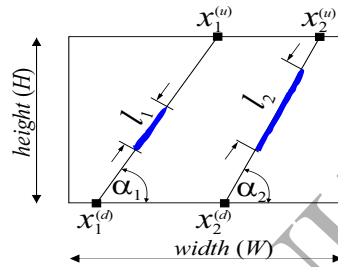


Figure 11: Parameters of the two samples of furrows

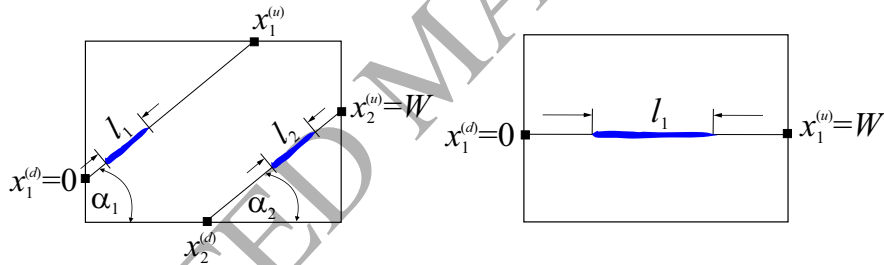


Figure 12: Parameters of the furrows which lie at an specific angle  $\alpha$ .

The value of each element of the vector  $\mathbf{L}$  is normalized to the interval  $[0,1]$  using the formula:  $val^{new} = val/max$ . The value  $max$  for the parameter  $\alpha$  is  $180^\circ$ , because the coordinate  $x^{(u)}, x^{(d)}$  is equal to the width of the image, while the parameter  $l$  is equal to the length of the image's diagonal. The result of this parametrization of all the image's furrows is the set  $\mathbf{L}_i = [x_i^{(u)}, x_i^{(d)}, \alpha_i, l_i]$ , where  $i = 1, \dots, m$  is the vector representing the  $i$ th furrow, while  $m$  is the number of all furrows.

#### 4.5. Creation of the pattern

In the proposed method, personal identification takes place on the basis of the result of a comparison of the size, location and inclination of the

furrows found in a lip print image. During analysis of lip print images, a problem appears in that the location and size of the same furrow may differ in subsequent images obtained from the same person. There are cases where a given furrow may not be visible at all in one of the images. This problem arises from the lips' high flexibility and has been described in [41]. Fig. 13 shows the differences between corresponding fragments of two lip images taken from the same person.

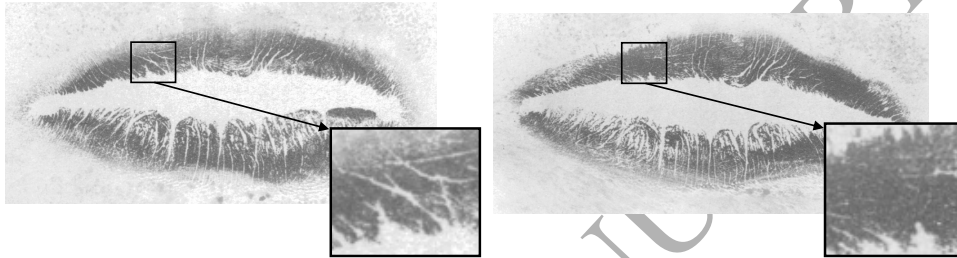


Figure 13: Two images of the lips belonging to the same person. In the left image there are furrows that are not visible in the right image.

To minimize the problem mentioned above, we propose a novel solution that consists of finding and analyzing only such furrows that occur in the largest number of images obtained from the same person, and of which the furrows' locations and inclinations are similar. A set of such furrows will be referred to in the remainder of this paper as a given person's lip pattern. The number of discovered furrows in a pattern is represented by the parameter  $k$ . A detailed description of the process of creating a lip pattern is presented here:

**Step 1.** Prepare the set  $\Omega = \{\Upsilon^1, \Upsilon^2, \dots, \Upsilon^N\}$  that contains  $N$  images of lips belonging to the person for whom the pattern is created. Set the value  $k$  representing the number of furrows to be included in the pattern. Set  $j = 1$ .

**Step 2.** Create a set of furrows by taking one furrow from each image in such a way that this set is unique. If it is not possible to create a new set of furrows, (it means that new matrices  $\mathbf{M}_j$  can not be formed), then go to **Step 5**. Based on the obtained set of furrows, create the matrix:

$$\mathbf{M}_j = [\mathbf{L}_a, \mathbf{L}_b, \dots, \mathbf{L}_n]^T, \quad (4)$$

where  $\mathbf{L}_a \in \Upsilon^1$ ,  $\mathbf{L}_b \in \Upsilon^2$ , ...,  $\mathbf{L}_n \in \Upsilon^N$ ,  
 $a = 1, 2, \dots, \#(\Upsilon^1)$ ,  $b = 1, 2, \dots, \#(\Upsilon^2)$ ,  $n = 1, 2, \dots, \#(\Upsilon^N)$ .

**Step 3.** Calculate the differences  $\psi_j$  between the individual furrows on the basis of which the matrix  $\mathbf{M}_j$  was created. A value of  $\psi_j = 0$  means that compared furrows are identical:

$$\psi_j = \|std(\mathbf{M}_j)\| \cdot len, \quad \psi_j \in [0, \infty), \quad (5)$$

where  $std(\mathbf{M}_j)$  is a vector of standard deviations calculated for each column of the matrix  $\mathbf{M}_j$ ,  $\|\cdot\|$  being a norm of the vector,  $len = ((1 - l_a) + (1 - l_b) + \dots + (1 - l_n))/n$ , and  $l_a, l_b, \dots, l_n$  are the lengths of the furrows being analyzed.

**Step 4.** Set  $j=j+1$  and return to **Step 2**.

**Step 5.** Out of all matrices  $\mathbf{M}_j$ , select the  $k$  matrices for which the smallest values of the difference  $\psi$  were obtained.

**Step 6.** For each of the  $k$  selected matrices  $\mathbf{M}_i$  average the values in its individual columns. The results create the vectors  $\bar{\mathbf{L}}_i$ ,  $i = 1, \dots, k$ . Finally, the set  $P = \{\bar{\mathbf{L}}_1, \bar{\mathbf{L}}_2, \dots, \bar{\mathbf{L}}_k\}$  forms the lip pattern.

**Step 7.** End algorithm.

The value of the difference  $\psi_j$  in eq. (5) indicates to what extent the values of the furrows' parameters are focused around their mean values. In addition, the parameter  $len$  was introduced which reduces the influence of long furrows on the value of  $\psi_j$ . Such furrows rarely occur in images, but they do better characterize an individual's lip. The principle of determining the difference  $\psi_j$  between the furrows in images is schematically shown in Fig. 14. In each image, the furrows being compared with each other are marked in black and by auxiliary arrows.

As mentioned earlier, patterns are determined separately for the upper and lower lip and will be designated as  $P_{up}$  and  $P_{down}$ , respectively.

#### 4.6. Personal Identification

Identification of an unknown lip print begins with its preparation in the manner described in Section 4.1. The resulting image is divided into its upper

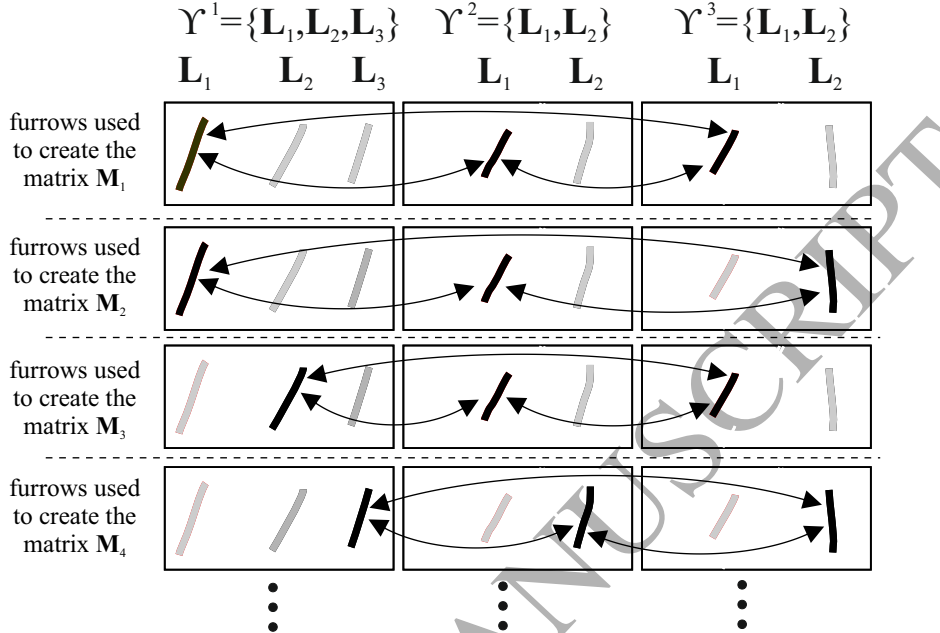


Figure 14: Determination of the similarity between furrows in lip print images. The furrows used to create the matrices  $M_j$  are marked in black and indicated by arrows.

and lower lips and then parameterized. As a result, two sets are obtained:  $\Upsilon_{up}$  containing the furrows of the upper lip and  $\Upsilon_{down}$  containing the furrows of the lower lip.

The sets  $\Upsilon_{up}$  and  $\Upsilon_{down}$  are compared with the patterns of the upper and lower lips, respectively, of all persons in the database. The method of comparison is the same for both lips. It will be described generally, without indicating the lip to which it applies. In practice, there can be a different number of furrows in the database's patterns compared to the image being identified. Therefore, the images are compared using the Czekanowski coefficient [42, 43] which allows for the comparison of two sets containing different amounts of data. This coefficient was appropriately modified and can be expressed by the following formula:

$$d(P^j, \Upsilon^*) = \sum_{i=1}^k \min (\|\bar{L}_i^j - L_1^*\|, \dots, \|\bar{L}_i^j - L_m^*\|), \quad (6)$$

where  $P^j = \{\bar{L}_1^j, \bar{L}_2^j, \dots, \bar{L}_k^j\}$  is the pattern of the  $j$ th person containing  $k$

furrows, while  $\Upsilon^* = \{\mathbf{L}_1^*, \mathbf{L}_2^*, \dots, \mathbf{L}_m^*\}$  is the image of lips of the person being identified, containing  $m$  furrows.

As mentioned earlier, furrows are compared separately for the upper and lower lips. From (6) we obtain two values:  $d_{up}(P_{up}^j, \Upsilon_{up}^*)$  for upper and  $d_{down}(P_{down}^j, \Upsilon_{down}^*)$  for lower lip. By averaging the results, we determine the value  $\bar{d}(P^j, \Upsilon^*)$  which is treated as the result of the comparison between the two lips  $\Upsilon^*$  of the person being identified and the pattern of the  $j$ th reference lip print:

$$\bar{d}(P^j, \Upsilon^*) = \frac{1}{2}(d_{up}(P_{up}^j, \Upsilon_{up}^*) + d_{down}(P_{down}^j, \Upsilon_{down}^*)). \quad (7)$$

For identification, the image  $\Upsilon^*$  obtained from the person being identified is classified as coming from the person for whom the reference lip pattern  $\Upsilon^*$  shows the fewest differences, i.e. has the lowest value  $\bar{d}(P^j, \Upsilon^*)$ .

## 5. Experiments and results

### 5.1. Database

For obvious reasons, lip prints databases collected in forensic laboratories are not publicly available. Additionally, the lip datasets created by other authors [30] are also not available and can not be used in studies. For this reason, the authors have created a database comprising 350 lip prints obtained from 50 people (7 prints per person). Each image has a resolution of  $800 \times 400$ px (300dpi). The created database is available on request from the website <http://biometrics.us.edu.pl>.

### 5.2. Experiment 1

In the first experiment, the impact of the furrows' directions on the system's accuracy was checked. A bar graph of the selected furrows' directions was constructed.

*Experimental Protocol:* Originally it was assumed that furrows of known direction will be analyzed at step  $\Delta = 1^\circ$  (Fig. 15 bar A). Observation has now shown that the step  $\Delta = 45^\circ$  is sufficient to detect differences in the accuracy of the identification system. The greater precision of measurement does not affect the personal identification results. Table 1 depicts the angular range of the analyzed furrows' directions. The bar graph from Fig. 15 shows that the accuracy of the system depends on the various ranges of the furrows' directions, which will be taken into account during the lip print analysis.

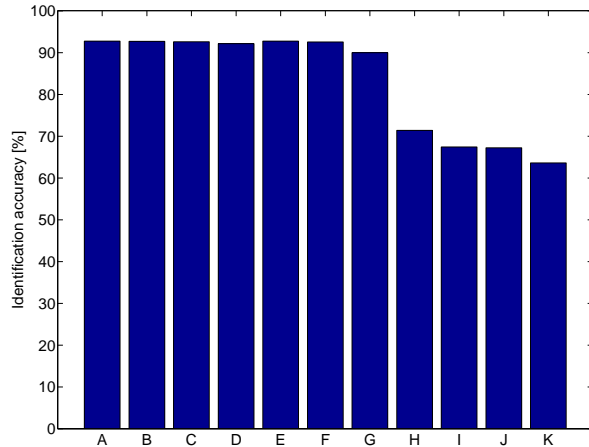


Figure 15: Accuracy of biometric system depends on angular changes of the lip furrows.

Table 1: Proposed furrows' angular changes in the experiment.

Bar name	$\Delta$	Angles
A	1°	0°, 1°, ..., 179°
B	10°	0°, 10°, ..., 170°
C	20°	0°, 20°, ..., 160°
D	30°	0°, 30°, ..., 150°
E	40°	0°, 40°, ..., 160°
F*)	45°	0°, 45°, 90°, 135°
G	50°	0°, 50°, 100°, 150°
H	60°	0°, 60°, 120°
I	70°	0°, 70°, 140°
J	80°	0°, 80°, 160°
K	90°	0°, 90°

\*) for clarity, this range can also be denoted as  $\{-45^\circ, 0^\circ, +45^\circ, 90^\circ\}$ , as previously.

*Results:* The results are presented in Table 2. From Fig. 15 it can be observed that, for the bar F, only four furrows' directions have been taken into consideration, ensuring a high accuracy level. For the bars A, B, C, D

and  $E$ , we obtain a similar accuracy of the system but with a greater variety of angles. From a complexity point of view this is not advantageous. Finally, in our experiments only the range  $\alpha \in \{-45^\circ, 0^\circ, 45^\circ, 90^\circ\}$  of the furrows' locations will be taken into account.

A similar strategy for the selection of angular grooves was proposed in [29]. In that work, the authors assumed that angular selection covers the prominent grooves, but this was stated without any proof, testing or literature review. In contrast to that work, our approach proposes an analysis of a wide angular range (Fig. 15). We show that various ranges of angular adjustments can be taken into account and the selection of angular ranges depends, mainly, on the time restrictions. It will also be demonstrated in Experiment 4.

### 5.3. Experiment 2

The purpose of the second experiment was to determine the effectiveness of the identification process. *Identification accuracy* is defined as the percentage of correctly recognized samples from the total number of the samples tested. Also examined was how the number of images used to create a pattern affected the personal identification effectiveness. This is important since the use of too many images when creating a pattern may extend the time taken to create it without any increase in the effectiveness of the identification. In addition, the impact of the parameter  $k$ , which specifies the number of furrows in the created pattern, on the identification accuracy was tested.

*Experimental Protocol:* The main purpose of this experiment was to determine the accuracy of the system in a closed-set identification process, such that all persons being identified are contained in the source database. It should be noted that, also, an open-set approach can be adopted. In such a case, an additional identification threshold would have to be introduced. This identification mode was not taken into consideration. In the next part of this paper, this will be demonstrated by means of the CMC curves (Fig. 17). Here, identification accuracy is checked using the following protocol. In the first stage, on the basis of four lip print images of a given person, their pattern image is created. These patterns, including a specified number of images, were created repeatedly, each time on the basis of a different set of images.

During the acquisition process, 7 lip prints images were prepared for each person. Using a random selection of 2 to 6 of these lip prints, each person's

lip pattern was then constructed. The remaining images were taken as test lip prints. For example, if 3 lip print images had been used to form the lip pattern, then 4 ( $7 - 3$ ) lip prints remained as test images. This procedure was repeated 20 times, following which the system's average accuracy was determined. The number of furrows for each lip of the lip pattern was selected by changing the parameter  $k$  (see Section 4.5). This parameter was changed from 5 to 30, in increments of 5. The optimal number of furrows for the lip print was determined separately for the upper and lower lip, as was the optimal number of lip prints for that person. This was repeated for each person's lip prints in the dataset. It should also be noted that during our research, blurred lip prints were tested. Such types of damaged lip prints were randomly created on the basis of personal lip images from the database. This is depicted in Fig. 18 and will be presented later.

Next, the system performance was checked using a cross-validation procedure. In this procedure, lip print images from the database were compared with a pattern from a given person. This comparison is performed on the basis of the formula (7).

*Results:* Results are presented in Fig. 16 and Table 2, along with the standard deviations of the identification accuracy. In Fig. 16 the highest accuracy values are shown for different numbers of lip print images, in points presented as tuples (accuracy, no of upper furrows, no of lower furrows).

Table 2 presents the same results as in Fig. 16, but here additionally are presented accuracy deviations. This helps to select the optimal values of the number of furrows that should be analyzed and the number of lip prints that should be taken into account for the determination of the accuracy of the system. It can be seen that the best effectiveness was obtained where the pattern included 15 furrows selected from the upper and 15 furrows from the lower lip. The results presented in Table 2 also indicate that, along with an increase in the number of images necessary to create the pattern, the effectiveness of classification increases too. However, it can be noted that the results obtained for four, five and six images are similar and are at a identification accuracy level of approximately 92.7%.

Considering the effectiveness of the method and its time performance, it has been assumed that the best personal identification level will be reached for the best matched  $k = 15$  pattern furrows located on the four images of a given person. The final decision about the influence of the number of furrows and lip print images on the accuracy of the recognition system should also take into account the time taken for the operation.

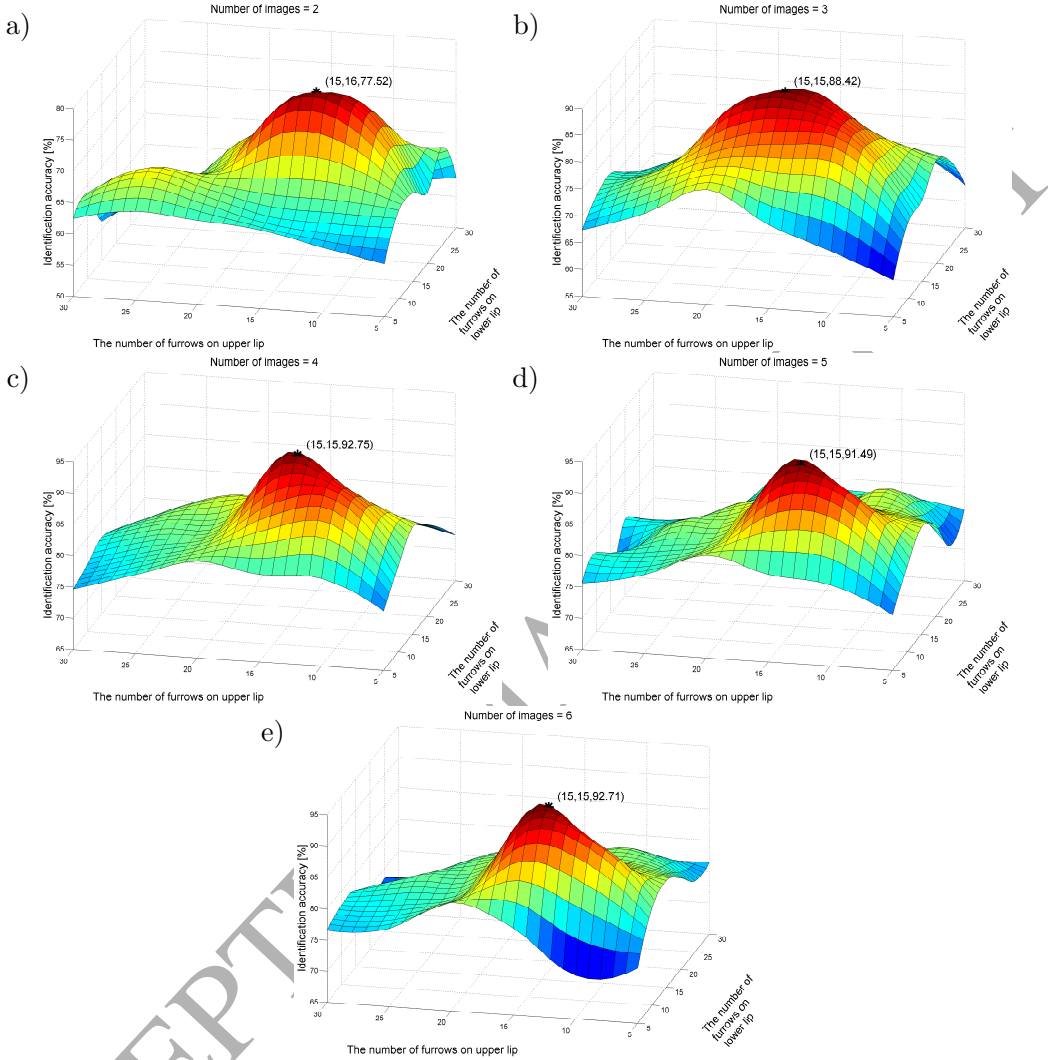


Figure 16: Identification system accuracy for different numbers of lip print images and for different numbers of analyzed furrows on the upper and lower lips. The highest black point indicates three parameters: (no of furrows on the upper lip, no of furrows on the lower lip, system accuracy).

The average time for the creation of a lip pattern was also measured. The results are presented in Table 3. These measurements confirm that the number furrows and lip print images was correctly established. The time for processing is significantly greater when the number of images taken for

pattern construction exceeds 4 (Table 3).

Table 2: The identification accuracy [%] depending on the number of images used to create the pattern and the number of furrows  $k$  in the pattern.

Number of images	The number of furrows on each lip of the pattern					
	$k=5$	$k=10$	$k=15$	$k=20$	$k=25$	$k=30$
2	58.58	75.17	77.55	67.78	57.48	53.11
	$\pm 4.74$	$\pm 6.26$	$\pm 5.23$	$\pm 5.31$	$\pm 4.45$	$\pm 4.20$
3	62.22	81.25	88.95	76.421	70.05	59.66
	$\pm 4.72$	$\pm 6.27$	$\pm 6.94$	$\pm 5.73$	$\pm 5.11$	$\pm 4.89$
4	74.96	88.72	92.73	82.33	77.12	68.18
	$\pm 5.00$	$\pm 6.47$	$\pm 6.42$	$\pm 5.54$	$\pm 5.56$	$\pm 4.89$
5	73.31	88.87	91.08	81.11	75.00	68.26
	$\pm 4.44$	$\pm 6.36$	$\pm 5.04$	$\pm 4.76$	$\pm 6.02$	$\pm 4.32$
6	74.21	89.43	92.66	80.99	74.91	68.70
	$\pm 5.41$	$\pm 6.50$	$\pm 6.89$	$\pm 5.60$	$\pm 4.88$	$\pm 3.98$

Table 3: Dependence of the time [s] required for creating the pattern on the number of images used for its creation.

Number of images	The number of furrows on each lip of the pattern					
	$k=5$	$k=10$	$k=15$	$k=20$	$k=25$	$k=30$
2	2.5	2.7	2.8	2.9	3.2	3.3
	$\pm 0.22$	$\pm 0.18$	$\pm 0.21$	$\pm 0.25$	$\pm 0.23$	$\pm 0.29$
3	3.6	4.2	4.5	4.8	5.4	6.1
	$\pm 0.30$	$\pm 0.43$	$\pm 0.44$	$\pm 0.45$	$\pm 0.60$	$\pm 0.72$
4	4.8	8.2	8.4	10.3	13.0	15.4
	$\pm 0.66$	$\pm 0.85$	$\pm 0.77$	$\pm 1.21$	$\pm 1.12$	$\pm 1.76$
5	6.3	38.0	109.0	128.0	187.8	251.6
	$\pm 0.65$	$\pm 3.80$	$\pm 11.84$	$\pm 15.00$	$\pm 22.52$	$\pm 33.71$
6	9.8	370.8	1292.0	1547.3	2334.1	3163.0
	$\pm 8.99$	$\pm 39.93$	$\pm 13.21$	$\pm 211.59$	$\pm 293.45$	$\pm 342.21$

#### 5.4. Experiment 3

In order to properly estimate the extent to which the use of lip patterns affect the effectiveness of this method, its results were compared with a method in which the identification was performed without building patterns.

*Experimental Protocol:* In this experiment, only a single reference image of a given person was selected and only a single image of the person's lip

print was obtained from each person. The test image was compared with the reference images of all persons in the database. This experiment, Experiment 3, did not include the step creating the lip pattern, so the number of furrows could not be determined to compare it with our use of our parameter  $k$ . Therefore, in order to determine the number of furrows, the  $p$  longest furrows on each of the lips were searched for in the image. Similar to previously, the longest furrows were designated by the Hough Transform. For each person, the comparisons were performed six times, each time with a different number  $p$  of longest furrows. After designating the  $p$  furrows, their parameters are determined in the same way as in the previous experiment. Like in Experiment 1, the best match belongs to the person for which the value  $\bar{d}$  (see eq. 7) was the smallest. It should be noted that, in this experiment, for a given  $p$  longest furrows, all their parameters ( $x_i^{(u)}, x_i^{(d)}, \alpha_i, l_i$ ) were also taken into consideration, similarly as for pattern creation. This has been discussed previously.

*Results:* The results of the experiment are shown in Table 4. The results presented in Table 2 and in Table 4 show that identification procedures that do not use pattern formation are more than 20% worse when compared to a method in which personal patterns were generated.

Table 4: The identification accuracy [%] method without pattern formation.

	The number of the longest furrows on each lip					
	$p=5$	$p=10$	$p=15$	$p=20$	$p=25$	$p=30$
Identification accuracy [%]	51.37 ± 4.66	65.05 ± 5.70	70.23 ± 6.48	62.07 ± 6.92	49.23 ± 4.45	42.62 ± 5.09

### 5.5. Experiment 4

In the next experiment, the Cumulative Match Characteristics (CMC) curves were determined. This is one of the measures of the effectiveness of an identification system. This characteristic allows for the determination of the probability that the person being identified is included in the set of selected  $n$ -candidates with the highest level of similarity to that person.

*Experimental Protocol:* This study was similar to that of Experiment 1, apart from the fact that Experiment 1 included the creation of patterns only on the basis of four images. Now we analyze a greater number of lip print images while simultaneously controlling the time taken for pattern creation (Table 3). The time complexity of this procedure is approximately  $O(n^2)$ , so

four images per pattern gives a reasonable processing time without any loss of recognition quality. This would further significantly reduce computation time.

The CMC curves were determined both for the method that used patterns for identification and for the method in which identification took place through a direct comparison of prints. The CMC curves were determined for different numbers of furrows on the lips. The CMC curves (Fig. 17); obtained for the pattern identification method show that an identification rate = 1 has been obtained, already, for a set of three candidates with an analysis of 15 furrows on each lip. For the method of identification that does not use patterns, the set of candidates should be increased to at least nine people.

### 5.6. Experiment 5

In practice, lip images acquired at a crime scene may be of poor quality, e.g. they can be indistinct, blurred or incomplete, which means that some their fragments may be not visible. Here, such unavailable regions were randomly selected. Thus, the purpose of Experiment 5 was to determine the effectiveness of the method in the case of an analysis of such images. In practice, contaminated or incomplete images do occur.

*Experimental Protocol:* The studies were carried out by creating a lip pattern on the basis of four complete images of good quality. The 15 furrows on each of the lips were analyzed. The test prints were “adequately” prepared, i.e. they were subjected to blurring, the addition of noise and to the blanking out of various fragments. Three levels of each of the aforementioned operations have been adopted in our studies: low, medium and high.

Noising was generated with three density of noise (*salt & pepper* type)  $g=0.05$  (low),  $g=0.10$  (medium) and  $g=0.15$  (high). Blurring of the lip print image was performed with parameter  $radius=2$  (low),  $radius=4$  (medium) and  $radius=6$  (high). During our studies, 25% to 75% of the area of the lips images was blanked out. The total area of the lips was calculated based on the region of the lips shown in Fig. 5. A sample of arbitrary selected images obtained as a result of the aforesaid three operations are shown in Fig. 18.

*Results:* The results of the studies are presented in Tables 5,6 and 7.

A comparison of the results from Tables 5,6, 7 with the results from Table 2 shows that degradation of the image adversely affects identification

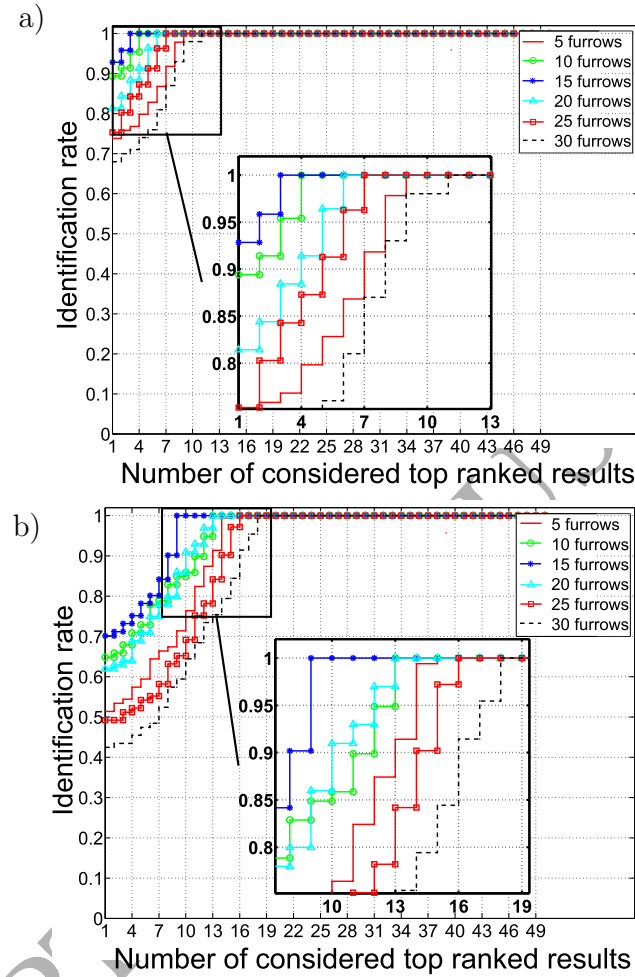


Figure 17: The CMC curves obtained for: a) the method based on the lip pattern, b) for the method without the use of the lip pattern.

effectiveness. This is consistent with our expectations, but the analysis of the impact of the individual operations on the end result deserves special attention. The proposed method uses the Hough transformation for the extraction of furrows, a process highly resistant to image noise, while less resistant to blurring. Therefore, the introduction of a low level of blurring caused a reduction in the identification effectiveness of approximately 10%, a medium level of blurring by approximately 20%, while in the case of a high level of blurring the identification effectiveness decreased significantly by over

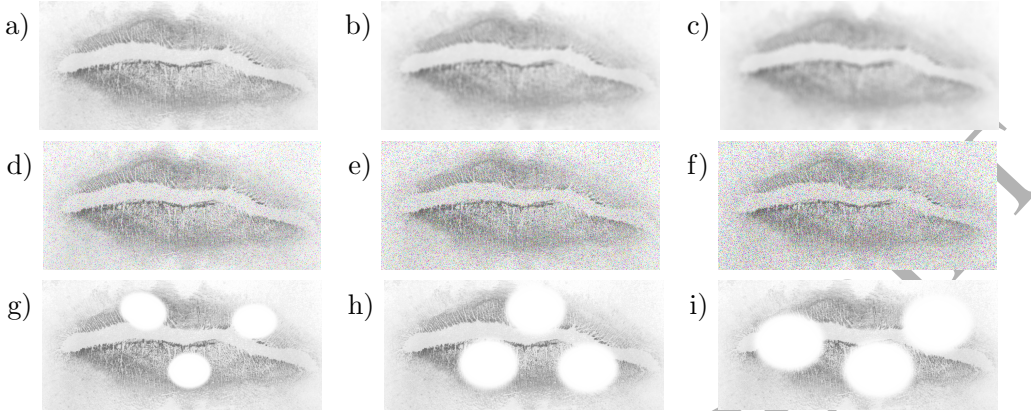


Figure 18: A sample image subjected to various degrees of blurring (a-c), noise (d-f) and blanking out of its fragments (g-i). In practice, these regions are randomly selected.

Table 5: The impact of blurring on identification accuracy [%].

low level of blurring (radius=2)	medium level of blurring (radius=4)	high level of blurring (radius=6)
81.00	68.47	28.69
± 6.07	± 4.15	± 2.16

60%. This is due to the fact that in the case of a very high level of blurring the furrows are almost invisible, which in turn hinders their extraction.

Our analysis of the impact of noise shows that noise causes only a slight decrease (by approximately 3%) in the effectiveness of the identification. In the case of a high level of noise, the decrease in the effectiveness of the identification was approximately 27%. Depending on the size of the area blanked out, the identification effectiveness ranged from 82.76% to 45.30%. The operation of blanking out certain areas differs from the previous operations of blurring and noise, because it does not degenerate all the furrows in the image. Even with 75% of the area of the lips blanked out, certain furrows are still visible, which enables their extraction and subsequent analysis.

## 6. Methodological point of view

In our approach we propose a lip print recognition strategy in which machine learning techniques are not needed. Thus the classifier's learning

Table 6: The impact of the noise on identification accuracy [%].

low noise level ( $g=0.05$ )	medium noise level ( $g=0.10$ )	high noise level ( $g=0.15$ )
88.95	81.44	65.22
$\pm 6.33$	$\pm 6.71$	$\pm 4.78$

Table 7: The impact of blanking out a fragment of the image on identification accuracy [%].

small area blanked out (25%)	medium area blanked out (50%)	large area blanked out (75%)
82.76	64.76	45.30
$\pm 6.46$	$\pm 3.81$	$\pm 3.21$

process can be eliminated. To the best of our knowledge, this is the best solution for lip print-based biometrics.

In machine learning methods, a features space needs to be formed and the features ordered according to some fixed criterion. The ordered features form a vector and are then classified. The human mouth plays an important role in eating, drinking, breathing and speaking, so is very flexible. For this reason, it is practically impossible to obtain any successive identical lip imprints, even from the same person. In the case of lip prints, features (here furrows) can be visible on one imprint whereas they can be invisible, deformed or shifted on another. This means that feature vectors can have various lengths, which is contrary to the assumption that vectors being classified should have the same length [44, 45, 46, 47]. Despite this, in this paper we also show a lip print identification approach based on popular machine learning classification algorithms: Random Tree, J48, kStar, Hoeffding Tree, Ridor and  $k$ -NN [37]. In this approach, we find  $p$  longest furrows on each lip image and then parameterize them. Furrow length was a unique parameter which allowed us to select the number of furrows that was appropriate but, at the same time, the same on all images. For other parameters, for example for angular range of the furrows, this was impossible, because the number of furrows with a given angle can be different in various images.

The obtained vectors consist of the elements shown on Fig. 11 and Fig. 12 in Section 4.5. Next, all vectors of a given person are sorted with respect to the value of a selected furrow feature ( $x^{(d)}, x^{(u)}, \alpha, l$ ) and sequentially merged into one feature vector. This approach ensures that the obtained feature

vector length is always constant. All coordinates (features) of the feature vector remain, at all times, appropriately ordered. Table 8 includes various classifiers' accuracies obtained for the same collection of features as in the previous experiments, but with the use of a classifiers' learning procedure. Comparing the results in Table 8 with those of Table 3 (for  $k = 15$  furrows obtained from 4 lip print images) it can be observed that our lip pattern based approach always returned significantly higher accuracy than any method that used machine learning techniques, no matter how many furrows had been designated. In both experiments - with (Table 8) and without (Table 2) a learning procedure - the same database was employed.

Table 8: Lip print identification accuracy for various learning-based classifiers and various numbers of longest furrows, without pattern creation

sorting with respect to:	Random Tree	J48	kStar	Hoeffding Tree	Ridor	$k$ -NN
$p = 5$ longest furrows on each lip						
$x^{(d)}$	11.24	8.34	60.38	17.24	7.10	31.33
$x^{(u)}$	8.48	2.90	53.00	18.81	5.10	27.95
$\alpha$	3.95	6.62	50.67	16.38	3.10	26.48
$l$	6.05	5.89	42.67	12.48	0.74	19.95
$p = 10$ longest furrows on each lip						
$x^{(d)}$	17.24	15.34	60.38	26.24	12.10	33.33
$x^{(u)}$	15.48	14.90	57.00	25.81	3.10	34.95
$\alpha$	12.95	11.62	57.67	18.38	8.10	29.48
$l$	13.05	10.89	51.67	18.48	8.24	19.95
$p = 15$ longest furrows on each lip						
$x^{(d)}$	25.24	25.24	72.38	35.24	18.10	43.33
$x^{(u)}$	20.48	21.90	70.00	33.81	18.10	40.95
$\alpha$	5.24	11.90	16.67	12.86	6.19	7.62
$l$	19.05	19.05	56.67	30.48	15.24	30.95
$p = 20$ longest furrows on each lip						
$x^{(d)}$	14.24	16.34	58.38	28.24	5.10	31.33
$x^{(u)}$	9.48	15.90	63.00	22.81	11.10	31.95
$\alpha$	13.95	12.62	53.67	17.38	5.10	33.48
$l$	6.05	14.89	51.67	17.48	10.24	23.95
$p = 25$ longest furrows on each lip						
$x^{(d)}$	14.24	11.34	56.38	17.24	2.10	30.33
$x^{(u)}$	6.48	6.90	55.00	22.81	1.10	25.95
$\alpha$	1.95	4.62	55.67	12.38	1.10	27.48
$l$	5.05	4.89	44.67	15.48	1.02	18.95
$p = 30$ longest furrows on each lip						
$x^{(d)}$	18.24	17.34	68.38	30.24	10.10	34.33
$x^{(u)}$	13.48	12.90	62.00	29.81	12.10	28.95
$\alpha$	15.95	6.62	62.67	26.38	14.10	29.48
$l$	15.05	10.89	52.67	22.48	5.24	24.95

## 7. Comparative studies

As has been previously demonstrated, the proposed lip print identification strategy has been evaluated on a database comprised of 350 lip prints (similar to Fig.1) obtained from 50 people with 7 prints taken per person. Acquisition of lip print images was presented in Section 2. Reliable comparative studies of the various techniques in which lip imprints have been employed require a uniform comparison technique. In our approach, we computed the method's accuracy, but in other papers others factors such as FAR, FRR, EER as well as ROC curves were proposed. To the best of our knowledge, Table 9 is the first announcement in the literature in which results of the each of the most representative strategies and their systematic accuracies have been stated.

Experimental results in Table 9 are uniformly presented in terms of accuracy. When the results of other authors are stated in terms of the EER factor, we re-presented this as an accuracy value, because accuracy in relation to EER (Equal Error Rate) is nothing but  $(100 - \text{EER})$  [48, 49].

Table 9: A comparison of our results with the most representative achievements from the literature.

Authors and works	Accuracy [%]	Methods	Database description
Our method	92.73	Creation of lip patterns	350 lip prints obtained from 50 people (7 prints per person)
Bhattacharjee S. et al. [29]	96.0	Statistical method	20 lip prints from 4 persons
Porwik P. et al. [50]	88.5	DTW algorithm + voting system	120 lip prints (30 persons, 4 lip prints from each person)
Wrobel K. et al. [13]	85.1	Section comparison	45 lip prints (15 persons, 3 lip prints from each person)
Smacki L. et al. [51]	78.8	DTW algorithm	120 lip prints (30 persons, 4 lip prints from each person)
Wrobel K. et al. [31]	77.0	Bifurcation analysis	120 lip prints (30 persons, 4 lip prints from each person)

Table 9 shows the performance of different systems over different numbers of subject individuals. Other systems contain fewer objects, which means less variety. Since we are working on a reasonably large database, the performance of the proposed system seems to be quite stable when compared to the results of other experiments. Second, systems presented in [29] reported

that the Euclidean distance was used as their statistical measure. In our approach we instead propose Czekanowski's coefficient - see eqs. (6), (7). This coefficient can be used when datasets have different numbers of elements. It is especially important in cases in which lip prints are blurred or corrupted, for example. Thus, our approach seems to be more precise.

## 8. Conclusions

No system of lip-based automatic identification can fully replace the work of forensic technicians or take decisions for them, but it can successfully facilitate and accelerate their work. To a large extent, our proposed method seems to meet both of these needs.

Conclusions and observations concerning this new personal identification method based on lip patterns, as proposed in this paper, can be summarized as follows:

- This method enables an effective identification of persons based on their lip prints. The best identification accuracy equals 92.73% and the CMC curve shows a rank-three identification rate of 100%. The values we have obtained are higher than any previously known methods based on the analysis of lip prints [30].
- The use of lip patterns created from several lip prints allowed an increase in the effectiveness of identification by approximately 20% as compared to the approach in which patterns were not created. This proves the validity of the approach proposed in this paper, an approach based on building lip patterns.
- In the proposed method, only four reference prints are sufficient to create a lip pattern.
- The best identification results were obtained by utilizing 15 furrows on each lip of the pattern.
- The high efficiency of this method (over 80%) in the analysis of degraded lip prints, along with the measured identification times, together indicate that this method can have practical applications in the forensic domain.

The problem of the identification of lip prints described in this paper is difficult and does require further study. Future research will include the use of various types of classifiers for comparing the lip's furrows. The most important future tasks will include the development of a system that uses

high resolution images, which analyses not only the global features of the lips but also the furrows located on them. The use of our work as part of a multi-biometric method also appears as an interesting possibility.

## Appendix A.

---

**Algorithm 1:** Determination of the region between the lower and upper lips.

---

**Data:** Binary lip print image  $I(x, y)$  of size  $Width \times Height$ .  
**Result:** Binary image  $I(x, y)$  on which all the pixels not lying between the lips are set to black.

```

1 for  $j = 1$  to  $Width$  step = 1 do
    // Set pixels above mouth as black pixels
    2  $i = 1;$ 
    3 while ( $I(j, i) \neq$  Black pixel) and ( $i \neq Height$ ) do
        4      $I(j, i) =$  Black pixel;
        5      $i = i + 1;$ 
    // Set pixels below mouth as black pixels
    6      $i = Height;$ 
    7     while ( $I(j, i) \neq$  Black pixel) and ( $i \neq 1$ ) do
        8          $I(j, i) =$  Black pixel;
        9          $i = i - 1;$ 

```

---

**Algorithm 2:** Length counting algorithm.

---

**Data:**  $I(x, y)$  – binary input image of lip furrows of size  $Width \times Height$ ;  $Tmp(x, y)$  – temporary matrix of size  $Width \times Height$ ;  $l_T$  – minimal size of single furrow in pixels.

**Result:**  $I(x, y)$  – binary image with lip furrows size greater than or equal to  $l_T$  pixels, where the value  $l_T$  was established by the PSO strategy.

```

1   $Prev = I(1, 1);$ 
2   $Tmp = I;$ 
   // Calculating the furrows size
3  for  $y = 2$  to  $Height - 1$  step = 1 do
   // Determining the direction of analysis for a given row
4    if  $(y \bmod 2) = 1$  then
5       $x_{start} = 2; x_{end} = Width - 2; x_{step} = 1;$ 
6    else
7       $x_{start} = Width - 2; x_{end} = 2; x_{step} = -1;$ 
   // Numbering of the points on the furrow
8    for  $x = x_{start}$  to  $x_{end}$  step =  $x_{step}$  do
9       $max = 0;$ 
10     if  $I(x, y) = Black\ pixel$  then
11       for  $dx = -1$  to 1 step = 1 do
12         if  $Tmp(x + dx, y - 1) > max$  then
13            $max = Tmp(x + dx, y - 1);$ 
14       if  $Prev > max$  then
15          $max = Prev;$ 
16        $Tmp(x, y) = max + 1;$ 
17        $Prev = Tmp(x, y);$ 
   // Distribution of the calculated furrow size to other furrow pixels
18   $Prev = Tmp(Width, Height - 1);$ 
19  for  $y = Height - 2$  to -1 step = -1 do
20    if  $(y \bmod 2) = 1$  then
21       $x_{start} = Width - 2; x_{end} = 2; x_{step} = -1;$ 
22    else
23       $x_{start} = 2; x_{end} = Width - 2; x_{step} = 1;$ 
24    for  $x = x_{start}$  to  $x_{end}$  step =  $x_{step}$  do
25       $max = Tmp(x, y);$ 
26      if  $Tmp(x, y) > 0$  then
27        for  $dx = -1$  to 1 step = 1 do
28          if  $Tmp(x + dx, y + 1) > max$  then
29             $max = Tmp(x + dx, y + 1);$ 
30        if  $Prev > max$  then
31           $max = Prev;$ 
32         $Tmp(x, y) = max;$ 
33         $Prev = Tmp(x, y);$ 
   // Elimination of furrows with size smaller than  $l_T$ 
34  for  $y = 1$  to  $Height$  step = 1 do
35    for  $x = 1$  to  $Width$  step = 1 do
36      if  $Tmp(x, y) \geq l_T$  then
37         $I(x, y) = Black\ pixel;$ 
38      else
39         $I(x, y) = White\ pixel;$ 

```

---

## References

- [1] A. Castello, M. Alvarez-Segui, F. Verdu, Luminous lip-prints as criminal evidence, *Forensic Science International* 155 (23) (2005) 185 – 187.
- [2] M. A. Segui, M. M. Feucht, A. C. Ponce, F. A. Pascual, Persistent lipsticks and their lip prints: new hidden evidence at the crime scene, *Forensic Science International* 112 (1) (2000) 41 – 47.
- [3] M. Newton, *The Encyclopedia of crime scene investigation, Facts on File Crime Library*, Facts On File, Incorporated, 2007.
- [4] K. Suzuki, Y. Tsuchihashi, A new attempt of personal identification by means of lip print, *Canadian Society of Forensic Science Journal* 4 (4) (1971) 154–158.
- [5] Y. Tsuchihashi, Studies on personal identification by means of lip prints, *Forensic Science* 3 (1974) 233 – 248.
- [6] J. Kasprzak, Possibilities of cheiloscopy, *Forensic Science International* 46 (1) (1990) 145 – 151.
- [7] R. Prabhu, A. Dinkar, V. Prabhu, P. Rao, Cheiloscopy: revisited, *Journal of Forensic Dental Sciences* 4 (1) (2012) 47–52.
- [8] M. H. A. Aziz, F. M. B. E. Dine, N. M. Saeed, Regression equations for sex and population detection using the lip print pattern among egyptian and malaysian adult, *Journal of Forensic and Legal Medicine* 44 (2016) 103 – 110.
- [9] N. Kapoor, A. Badiye, A study of distribution, sex differences and stability of lip print patterns in an indian population, *Saudi Journal of Biological Sciences* 24 (6) (2017) 1149 – 1154.
- [10] H. Utsuno, T. Kanoh, O. Tadokoro, K. Inoue, Preliminary study of post mortem identification using lip prints, *Forensic Science International* 149 (23) (2005) 129 – 132.
- [11] J. Dineshshankar, N. Ganapathi, T. Yoithaprabhunath, T. Maheswaran, M. Kumar, R. Aravindhan, Lip prints: Role in forensic odontology, *Journal of Pharmacy And Bioallied Sciences* 5 (5) (2013) 95–97.

- [12] A. Becue, C. Champod, Fingermarks and other body impressions— areview july 2013–july 2016, in: 18th International Forensic Science Managers Symposium, At Lyon (France), 2016, p. 48.
- [13] K. Wrobel, R. Doroz, M. Palys, A method of lip print recognition based on sections comparison, in: Biometrics and Kansei Engineering (ICBAKE), 2013 International Conference on, 2013, pp. 47–52.
- [14] S. K. Bandyopadhyay, S. Arunkumar, S. Bhattacharjee, Feature extraction of human lip prints, *Journal of Current Computer Science and Technology* 2(1) (2012) 1–8.
- [15] A. Danielis, D. Giorgi, M. Larsson, T. Strmberg, S. Colantonio, O. Salvetti, Lip segmentation based on lambertian shadings and morphological operators for hyper-spectral images, *Pattern Recognition* 63 (2017) 355 – 370.
- [16] T. H. N. Le, M. Savvides, A novel shape constrained feature-based active contour model for lips/mouth segmentation in the wild, *Pattern Recognition* 54 (2016) 23 – 33.
- [17] K. Wrobel, R. Doroz, P. Porwik, J. Naruniec, M. Kowalski, Using a probabilistic neural network for lip-based biometric verification, *Engineering Applications of Artificial Intelligence* 64 (2017) 112–127.
- [18] E. Gomez, C. M. Travieso, J. C. Briceno, M. A. Ferrer, Biometric identification system by lip shape, in: Security Technology, 2002. Proceedings. 36th Annual 2002 International Carnahan Conf.on, 2002, pp. 39–42.
- [19] C. M. Travieso, J. Zhang, P. Miller, J. B. Alonso, Using a Discrete Hidden Markov Model Kernel for lip-based biometric identification, *Image and Vision Computing* 32 (12) (2014) 1080 – 1089.
- [20] J. O. Kim, W. Lee, J. Hwang, K. S. Baik, C. H. Chung, Lip print recognition for security systems by multi-resolution architecture, *Future Generation Computer Systems* 20 (2) (2004) 295 – 301.
- [21] R. S. Choras, *Lip-prints feature extraction and recognition*, Springer Berlin Heidelberg, Berlin, Heidelberg, 2011, pp. 33–42.

- [22] M. Choras, The lip as a biometric, *Pattern Analysis and Applications* 13 (1) (2010) 105–112.
- [23] S. Bakshi, R. Raman, P. K. Sa, Lip pattern recognition based on local feature extraction, in: 2011 Annual IEEE India Conference, 2011, pp. 1–4.
- [24] C. M. Travieso, J. Zhang, P. Miller, J. B. Alonso, M. A. Ferrer, Bimodal biometric verification based on face and lips, *Neurocomputing* 74 (1415) (2011) 2407 – 2410.
- [25] H. E. Cetingul, E. Erzin, Y. Yemez, A. M. Tekalp, Multimodal speaker/speech recognition using lip motion, lip texture and audio, *Signal Process.* 86 (12) (2006) 3549–3558.
- [26] M.-I. Faraj, J. Bigun, Audiovisual person authentication using lip-motion from orientation maps, *Pattern Recognition Letters* 28 (11) (2007) 1368 – 1382, advances on Pattern recognition for speech and audio processing.
- [27] K. Wrobel, P. Porwik, R. Doroz, Effective lip prints preprocessing and matching methods, in: Proceedings of the 9th International Conference on Computer Recognition Systems CORES 2015, Wroclaw, Poland, 25–27 May, 2015, pp. 347–357.
- [28] L. Smacki, K. Wrobel, Lip print recognition based on mean differences similarity measure, Springer Berlin Heidelberg, Berlin, Heidelberg, 2011, pp. 41–49.
- [29] S. Bhattacharjee, S. Arunkumar, S. K. Bandyopadhyay, Personal identification from lip-print features using a statistical model, *International Journal of Computer Applications* 55(13) (2012) 30–34.
- [30] L. Smacki, Latent lip print identification using fast normalized cross-correlation, in: Biometrics and Kansei Engineering (ICBAKE), 2013 International Conference on, 2013, pp. 189–192.
- [31] K. Wrobel, R. Doroz, M. Palys, Lip print recognition method using bifurcations analysis, in: Intelligent Information and Database Systems - 7th Asian Conference, ACIIDS 2015, Bali, Indonesia, March 23-25, 2015, Proceedings, Part II, 2015, pp. 72–81.

- [32] J. Sauvola, M. Pietikinen, Adaptive document image binarization, *Pattern Recognition* 33 (2) (2000) 225 – 236.
- [33] R. Koprowski, P. Olczyk, Segmentation in dermatological hyperspectral images: dedicated methods, *Biomedical Engineering Online* 15 (97).
- [34] T. Pietzsch, S. Preibisch, P. Tomank, S. Saalfeld, Imglib2-generic image processing in java, *Bioinformatics* 28 (22) (2012) 3009–3011.
- [35] C. Lopez-Molina, B. D. Baets, H. Bustince, J. Sanz, E. Barrenechea, Multiscale edge detection based on gaussian smoothing and edge tracking, *Knowledge-Based Systems* 44 (2013) 101 – 111.
- [36] J. Kennedy, R. Eberhart, Particle swarm optimization, in: *Neural Networks, 1995. Proceedings., IEEE International Conference on*, Vol. 4, 1995, pp. 1942–1948 vol.4.
- [37] P. Porwik, R. Doroz, T. Orczyk, Signatures verification based on PNN classifier optimised by PSO algorithm, *Pattern Recognition* 60 (2016) 998 – 1014.
- [38] H. J. Escalante, M. Montes-y-Gómez, L. E. Sucar, Particle swarm model selection, *Journal of Machine Learning Research* 10 (2009) 405–440.
- [39] R. O. Duda, P. E. Hart, Use of the hough transformation to detect lines and curves in pictures, *Commun. ACM* 15 (1) (1972) 11–15.
- [40] J. Illingworth, J. Kittler, A survey of the hough transform, *Computer Vision, Graphics, and Image Processing* 44 (1) (1988) 87 – 116.
- [41] M. A. Eldomiati, R. I. Anwar, S. A. Algaidi, Stability of lip-print patterns: a longitudinal study of saudi females, *Journal of forensic and legal medicine* 22 (2014) 154158.
- [42] S. Cha, Comprehensive survey on distance/similarity measures between probability density functions, *International Journal of Mathematical Models and Methods in Applied Sciences* 1 (4) (2007) 300–307.
- [43] P. Porwik, R. Doroz, K. Wrobel, A new signature similarity measure, in: *World Congress on Nature and Biologically Inspired Computing*, Coimbatore, India, 2009, pp. 1021–1026.

- [44] B. Krawczyk, L. L. Minku, J. Gama, J. Stefanowski, M. Woźniak, Ensemble learning for data stream analysis: A survey, *Information Fusion* 37 (2017) 132 – 156.
- [45] Y. Zhang, J. Wu, C. Zhou, Z. Cai, Instance cloned extreme learning machine, *Pattern Recognition* 68 (2017) 52 – 65.
- [46] R. Tadeusiewicz, A. Horzyk, Man-Machine interaction improvement by means of automatic human personality identification, in: *Lecture Notes in Computer Science (including subseries Lecture Notes in Artificial Intelligence and Lecture Notes in Bioinformatics)*, Vol. 8838, 2014, pp. 278–289.
- [47] R. Burduk, P. Heda, Homogeneous Ensemble Selection - Experimental Studies, in: *Proceedings of International Multi-Conference on Advanced Computer Systems ACS 2016*, Miedzyzdroje, Poland, 19-21 October, 2016.
- [48] Writer-independent off-line signature verification using surroundedness feature, *Pattern Recognition Letters* 33 (3) (2012) 301 – 308.
- [49] P. Gupta, P. Gupta, Slap fingerprint segmentation, in: *2012 IEEE Fifth International Conference on Biometrics: Theory, Applications and Systems (BTAS)*, 2012, pp. 189–194.
- [50] P. Porwik, T. Orczyk, DTW and voting-based lip print recognition system, in: *Computer Information Systems and Industrial Management - 11th IFIP TC 8 International Conference, CISIM 2012, Venice, Italy, September 26-28, 2012. Proceedings*, 2012, pp. 191–202.
- [51] L. Smacki, K. Wrobel, P. Porwik, Lip print recognition based on DTW algorithm, in: *Third World Congress on Nature & Biologically Inspired Computing, NaBIC 2011, Salamanca, Spain, October 19-21, 2011*, 2011, pp. 594–599.

## Author Biography

**Krzysztof Wrobel** received his MSc and PhD from the University of Silesia in 1999 and 2006, respectively. He is currently working in the Computer Systems Department, Institute of Computer Science, University of Silesia. His current research interest areas are biometrics, digital image processing and computer graphics.

**Rafal Doroż** received the Ph.D. degree in computer science, from University of Silesia, Poland, in 2011. Currently, he is a Assistant Professor in the Computer Systems Department, University of Silesia. He main research interests are: biometrics, image processing, classifiers, and machine learning. He has published more than 50 papers in internationals journals and conference materials.

**Piotr Porwik** is a professor of computer science in the Computer System Department, Computer Science and Materials Science Faculty, Katowice, University of Silesia, Poland. At present he works as the head of Computer System Department at University of Silesia. Currently his scientific researches focus on biometrics, machine learning, classifier systems, image processing and medical imaging. He has published over 100 scientific papers, which were published in Polish and foreign journals as well as numerous national and international conference presentations and talks. He has also published 3 books and edited 5 books. He is also invited to many program committees of national and international conferences. Professor Porwik has been invited as a special guest or a speaker in conferences and congresses in Poland, Japan and India. Since 2007 he is the Editor-in-Chief of Journal of Medical Informatics & Technologies and Associate Editor in Int. J. of Biometrics. He is a reviewer of numerous international journals and fellowships including: Int. J. of Applied Mathematics and Computer Science, Int. J. of Pattern Recognition and Artificial Intelligence. J. of Medical Imaging and Health Informatics, Information Sciences, Neurocomputing, Biocybernetics and Biomedical Engineering, IEEE Transactions on Neural Networks and many others.

**Marcin Bernaś** received the M.Sc. degree from University of Silesia, Katowice, Poland in 2005 and Ph.D. degree from Silesian University of Technology in 2009. He currently works as an assistant professor at the Institute of Computer Science at University of Silesia. He is a reviewer for several renowned journals in computer science field and published over 30 scientific papers concerning wireless sensor networks, data mining, granular comput-

ing and decision support systems (classification and forecasting) for transport/medicine.

ACCEPTED MANUSCRIPT